FLOW PATTERN OF MHD CASSON NANOFLUID PAST A POROUS STRETCHING SHEET –A NUMERICAL APPROACH

M. Parvathi[1], J.S. Sukanya[2], B. Hari Babu[3], P. Roja[1], P. Chandra Reddy[1], M. Umamaheswar[1]

Article History: Received: 01.04.2023 **Revised:** 06.05.2023 **Accepted:** 21.06.2023

Abstract:

A numerical study has been performed to draw out the variations in the flow pattern of Casson nanofluid past a stretched porous sheet in conducting field. A non-Newtonian fluid namely Casson fluid with combination of copper nano particles is considered based on the importance of its high thermal properties when compared to regular fluids. To analyze temperature and concentration profiles, the parameters like thermal radiation, heat generation, radiation absorption, diffusion thermo effect, chemical reaction are also taken into account. The governed non-linear partial differential equations are changed into ordinary form of differential equations by employing suitable similarity transformations and then solved by Shooting technique using MAT lab. The results obtained are presented to explore the effects of various parameters through graphs and tables. It is noticed that both the velocities decrease with the increase in Casson parameter. The outcomes of this examination are mainly utilized in the factories in the preparation of thick juices and sauces.

Keywords: MHD, 3D flow, Chemical reaction, Radiation, Soret effect, Dufour effect, Casson Nanofluid, Porous medium, Stretching sheet.

[1]Department of Mathematics, Annamacharya Institute of Technology and Sciences (Autonomous) Rajampet -516126, A.P., India.
[2]Department of Mathematics, Srinivasa Ramanujan Institute of Technology (Autonomous) Ananthapuramu-515701, A.P., India
[3]Department of Mathematics, PACE Institute of Technology & Sciences (Autonomous), Ongole-523272, Andhra Pradesh, India

DOI: 10.31838/ecb/2023.12.6.66

Nomenclature:

a,b	stretching constants
β	Casson parameter
B_0	magnetic flux
C	concentration of the fluid
D_B	mass diffusion coefficient
f	dimensionless stream function
f'	dimensionless velocity
k_f	thermal conductivity of the fluid
kl	permeability of porous medium

k_{nf} effective thermal conductivity of the nanofluid
Kr chemical reaction parameter
k_s thermal conductivity of the solid
M magnetic parameter
Pr Prandtl number
Q_H heat generation parameter
Q_l radiation absorption parameter
q_r radiative heat flux
R radiation parameter
D_f Dufour number
Sc Schmidt number
S_0 Soret number
T temperature of the fluid
u, v, w fluid velocity components along x, y, z directions respectively

Subscripts:
nf nanofluid
f base fluid
s solid
∞ quantities at free stream
w quantities at wall

Greek symbols:
α_{nf} thermal diffusivity of nanofluid
μ_{nf} dynamic viscosity of nanofluid
ν_f kinematic viscosity
ρ_{nf} density of nanofluid
ϕ volume fraction
σ electrical conductivity
λ stretching ratio parameter
η similarity variable
β Casson fluid parameter
$(\rho C_p)_f$ heat capacitance of the fluid
$(\rho C_p)_{nf}$ heat capacity of the nanofluid
$(\rho C_p)_s$ heat capacitance of the solid
ρ_f density of the fluid
ρ_s density of the solid

1. INTRODUCTION

Over decades researchers are persistently working to boost heat transfer rate, thermal conductivity and at the same time trying to reduce frictional loss, pressure drop and pumping power for heat transfer fluid (HTF). A new type of HTF is engineered which provides improved thermal properties for heat transfer which is called as nanofluid. Nanofluid is a suspension of nanoparticles which is capable of heat transfer fluid in the heat transfer enhancement having a overabundance of applications due to superior thermal conductivity and rheological properties. Nanofluid is prepared by suspending a small quantity of nanoparticles in base fluids such as water, ethylene glycol etc. with or without stabilization techniques. The average size of nanoparticles is below 100 nm. Incorporation of nanoparticles dramatically improves the thermophysical properties of traditional heat transfer fluid which increase the heat transfer coefficient Choi [1]. These thermophysical properties are density, specific heat, thermal conductivity, and dynamic viscosity. The degree of enhancement of heat transfer depends on quantity of nanoparticles which is suspended in the base fluid. Metal oxides (Al_2O_3, CuO, TiO_2, ZnO, MgO, SiC etc.) are preferred as nanoparticles which have high thermal conductivity [2]. The convective flow and heat transfer of an incompressible viscous nanofluid past a semi-infinite vertical stretching sheet in the presence of a magnetic field is studied by Hamad [3]. Khan [4] illustrated the unsteady laminar boundary-layer flows of a nanofluid past a stretching sheet with thermal radiation in the presence of magnetic field.

Magnetohydrodynamics is the study of the magnetic properties and behavior of electrically conducting fluids. Examples of such magneto fluids include plasmas, liquid metals, salt water, and electrolytes. The term magnetohydrodynamics was first introduced by Alfven. He was the one who described the astrophysical phenomenon as an independent scientific discipline. But the official origin or the birth of non-compressible magnetohydrodynamic fluid is in the year 1936-37. Hartmann and Lazarus conducted a theoretical and experimental study of MHD fluid flow in ducts. In fluid dynamics, the influence of external magnetic field on magnetohydrodynamic (MHD) flow over a stretching sheet is very significant due to its applications in many engineering problems such as for purification of crude oil, paper production and glass manufacturing. A physiological process in human body can be deciphered by processes like MRI, NMRI and MRT, in which MHD plays an important role. Nayak et al. [5] presented a numerical simulation for three dimensional steady flow of nanofluids passing through an exponential stretching sheet in presence of magnetohydrodynamics . In three-dimensional flow Hayat et al. [6] discussed the soret and Dufour effects over an exponentially stretching surface with porous medium. Rosseland [7] studied the two-dimensional laminar, steady, incompressible flow past a flat plate subject to convective surface boundary condition, slip velocity in the presence of radiation. Sheikholeslami et al. [8] examined the natural convection of nanofluid flow and heat transfer in a cavity which is heated from below using the lattice Boltzmann method. Aurang Zaib et al. [9] analyzed the numerical solution of second law analysis for MHD Casson nanofluid past a wedge with activation energy and binary chemical reaction. Hayat et al. [10] investigates the steady three-dimensional flow of viscous nanofluid past a permeable shrinking surface with velocity slip and temperature jump. Nayak et al. [11] focuses on the influence of transverse magnetic field as well as thermal radiation on 3D free convective flow of nanofluid over a linear stretching sheet.

A Casson fluid can be defined as a shear thinning liquid which is assumed to have an infinite viscosity at zero rate of shear and a zero viscosity at an infinite rate of shear. Examples of Casson fluid are jelly, tomato sauce, honey, soap and concentrated fruit juices. Human blood is also an example of Casson fluid. Panigrahi et al. [12] analyzed the heat and mass transfer of MHD Casson nanofluid flow through a porous medium past a stretching sheet with Newtonian heating and chemical reaction. Besthapu et al. [13] employed mixed convection MHD flow of

a Casson Nanofluid over a nonlinear permeable stretching Sheet with viscous dissipation. Prasad et al. [14] investigated mixed convection heat transfer flow over a non-linear stretching surface with variable fluid properties. An Analytical Solution for boundary layer flow of a nanofluid past a stretching sheet is derived by Hassani et al. [15]. Steady, laminar boundary fluid flow from the non-linear stretching of a flat surface using a nanofluid has been investigated numerically by Rana et al. 16]. The magnetohydrodynamic (MHD) boundary layer flow of Casson fluid in the presence of nanoparticles is investigated by Hussain et al. [17]. Boundary layer flow of Casson nanofluid induced by non-linearly stretching surface is reported by Mustafa et al. [18].

The main aim of the present study is to investigate the flow pattern of Casson nanofluid in a conducing field in the presence of Dufour effect over a porous stretching sheet. The novel thing in this work is the inclusion of Casson parameter and diffusion- thermo effect for base work in the published paper.

Formulation of the problem:

Consider a three-dimensional, incompressible electrically conducting, free convective nanofluid flow past a permeable stretching porous sheet. Assume a transverse magnetic field of uniform strength B_0 is applied parallel to the z-axis followed by Nayak et al. [11]. The induced magnetic field and impressed electric field are ignored by assuming magnetic Reynolds number to be significantly small.

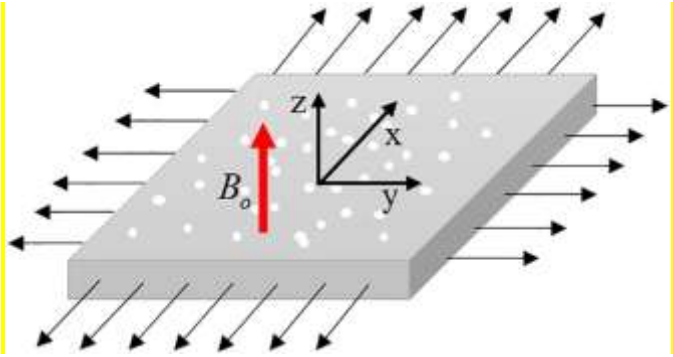

Fig.1Physcial representation of the problem

Under the above assumptions the governing equations of continuity, momentum, energy and species diffusion and Nayak et al. [11] are as follows:

$$\frac{\partial u}{\partial x}+\frac{\partial v}{\partial y}+\frac{\partial w}{\partial z}=0 \tag{1}$$

$$u\frac{\partial u}{\partial x}+v\frac{\partial u}{\partial y}+w\frac{\partial u}{\partial z}=\frac{1}{\rho_{nf}}\left\{\mu_{nf}\left(1+\frac{1}{\beta}\right)\frac{\partial^2 u}{\partial z^2}+(\rho\beta)_{nf}\,g(T-T_\infty)+(\rho\beta^*)_{nf}\,g(C-C_\infty)-\sigma B_0^2 u-\frac{\nu u}{k}\right\} \tag{2}$$

$$u\frac{\partial v}{\partial x}+v\frac{\partial v}{\partial y}+w\frac{\partial v}{\partial z}=\frac{1}{\rho_{nf}}\left\{\mu_{nf}\left(1+\frac{1}{\beta}\right)\frac{\partial^2 v}{\partial z^2}+(\rho\beta)_{nf}\,g(T-T_\infty)-(\rho\beta^*)_{nf}\,g(C-C_\infty)-\sigma B_0^2 v+\frac{\nu v}{k}\right\} \tag{3}$$

$$u\frac{\partial T}{\partial x}+v\frac{\partial T}{\partial y}+w\frac{\partial T}{\partial z}=\frac{k_{nf}}{(\rho C_p)_{nf}}\frac{\partial^2 T}{\partial z^2}-\frac{1}{(\rho C_p)_{nf}}\frac{\partial q_r}{\partial z}-Q(T-T_\infty)+Q_l(C-C_\infty)+\frac{D_B K_{nf}}{(\rho C_P)_{nf}}\frac{\partial^2 C}{\partial z^2} \tag{4}$$

$$u\frac{\partial C}{\partial x}+v\frac{\partial C}{\partial y}+w\frac{\partial C}{\partial z}=D_B\frac{\partial^2 C}{\partial z^2}+D_l\frac{\partial^2 T}{\partial z^2}-Kr^*(C-C_\infty) \tag{5}$$

subjected to the boundary conditions

$u = U_w(x) = ax, v = V_w(x) = bx$, $w = 0,\ T = T_w,\ C = C_w$ at z=0

$u \to 0,\ v \to 0,\ w \to 0,\ T \to T_\infty,\ C \to C_\infty$ as $z \to \infty$ (6)

where a > 0 and b > 0 for stretching sheet.

The properties of nanofluid are given by

$\rho_{nf} = (1-\phi)\rho_f + \phi\rho_s$, $(\rho C_p)_{nf} = (1-\phi)(\rho C_p)_f + \phi(\rho C_p)_s$, $(\rho\beta)_{nf} = (1-\phi)(\rho\beta)_f + \phi(\rho\beta)_s$,

$$\mu_{nf} = \frac{\mu_f}{(1-\phi)^{2.5}},\ K_{nf} = Kf\left\{\frac{K_s + 2K_f - 2\phi(K_f - K_s)}{K_s + 2K_f + 2\phi(K_f - K_s)}\right\} \quad (7)$$

The Rosseland approximation [12], the radiative heat term is given by

$$q_r = \frac{-4\sigma^*}{3k^*}\frac{\partial T^4}{\partial z},\ T^4 = 4T_\infty^3 T - 3T_\infty^4,\ \frac{\partial q_r}{\partial \bar{z}} = -16\frac{T_\infty^3\sigma^*}{3k^*}\frac{\partial^2 T}{\partial \bar{z}^2} \quad (8)$$

From (7), (8) and (4) energy equation is

$$u\frac{\partial T}{\partial x} + v\frac{\partial T}{\partial y} + w\frac{\partial T}{\partial z} = \frac{k_{nf}}{(\rho C_p)_{nf}}\frac{\partial^2 T}{\partial z^2} - \frac{16\sigma^* T_\infty^3}{(\rho Cp)_{nf}3k^*}\frac{\partial^2 T}{\partial z^2} - \frac{Q}{(\rho Cp)_{nf}}(T - T_\infty) + Q_l(C - C_\infty) \quad (9)$$

We consider the dimensionless variables as

$$u = axf'(\eta),\quad v = ayf'(\eta),\quad w = -(a\nu_f)^{1/2}(f(\eta) + g(\eta)),\quad \theta(\eta) = \frac{T - T_\infty}{T_w - T_\infty},\quad C(\eta) = \frac{C - C_\infty}{C_w - C_\infty},$$

$$\eta = \left(\frac{a}{\nu_f}\right)^{1/2} z \quad (10)$$

By using (7)-(10) Eqs. (2),(3),(8) and (5)

$$\left(1 + \frac{1}{\beta}\right)f''' + \varepsilon\left\{\varepsilon_1\left((f+g)f'' - (f')^2\right) + \left(\varepsilon_2\gamma_1\theta + \varepsilon_4\gamma_2 C - M - kl\right)f'\right\} = 0 \quad (11)$$

$$\left(1 + \frac{1}{\beta}\right)g''' + \varepsilon\left\{\varepsilon_1\left((f+g)g'' - (g')^2\right) - \left(\varepsilon_2\gamma_3\theta\varepsilon + \varepsilon_4\gamma_4 C + M - kl\right)g'\right\} = 0 \quad (12)$$

$$(A+R)\theta'' + \varepsilon_3\left(\mathrm{Pr}(f+g)\theta' + Q_l\right) - Q_H\theta + D_f C'' = 0 \quad (13)$$

$$C'' + Sc(f+g)C' + S_0 Sc\theta'' - ScKrC = 0 \quad (14)$$

with the boundary conditions

$f'(\eta) = 1,\ g'(\eta) = \lambda,\ f(\eta) = 0,\ g(\eta) = 0,\ \ \theta(\eta) = 1, C(\eta) = 1$ at $\eta = 0$

$f'(\eta) \to 0,\ g'(\eta) \to 0,\ \theta(\eta) \to 0,,\ C(\eta) \to 0$ as $\eta \to \infty$ (15)

where $\varepsilon = (1-\phi)^{2.5}$, $\varepsilon_1 = 1 - \phi + \phi\left(\frac{\rho_s}{\rho_f}\right)$, $\varepsilon_2 = 1 - \phi + \phi\left(\frac{(\rho\beta)_s}{(\rho\beta)_f}\right)$, $\varepsilon_3 = 1 - \phi + \phi\left(\frac{(\rho C_p)_s}{(\rho C_p)_f}\right)$,

$\varepsilon_4 = 1 - \phi + \phi\left(\frac{(\rho\beta^*)_s}{(\rho\beta^*)_f}\right)$, $M = \frac{\sigma B_0^2}{a\rho_f}$, $R = \frac{16\sigma^* T_\infty^3}{3k^* k_f}$, $\lambda = \frac{b}{a}$, $\gamma_1 = \frac{g\beta_f(T_w - T_\infty)}{au}$,

$$\gamma_2 = \frac{g\beta_f^*(C_w - C_\infty)}{au}, \quad \gamma_3 = \frac{g\beta_f(T_w - T_\infty)}{av}, \quad \gamma_4 = \frac{g\beta_f^*(C_w - C_\infty)}{av}, \quad kl = \frac{\nu_f}{ak\rho_f}, \quad Q_H = \frac{Q}{a(\rho Cp)_f},$$

$$Q_l = \frac{Q_l^*(C_w - C_\infty)}{a(T_w - T_\infty)}, \; Sc = \frac{\nu_f}{D_B}, \; S_0 = \frac{D_l(T_w - T_\infty)}{\nu_f(C_w - C_\infty)}, \; Kr = \frac{Kr^*}{a}, \; \Pr = \frac{\nu_f}{\alpha_f}, \; A = \frac{k_{nf}}{k_f} \tag{16}$$

The local skin friction co-efficient about x-axis is C_{fx} and y-axis C_{fy}, local Nusselt number Nu_x and local Sherwood number Sh_x are given by

$$C_{fx} = \frac{\tau_{wx}}{\rho_f U_w^2}, \; C_{fy} = \frac{\tau_{wy}}{\rho_f V_w}, \; Nu_x = \frac{xq_w}{k_f(T_w - T_\infty)} \text{ and } Sh_x = \frac{xq_m}{D_B(C_w - C_\infty)}$$

where the wall shear stresses along x-axis and y-axis of the stretching surface are $\tau_{wx} = \mu_{nf}\left(\frac{\partial u}{\partial z}\right)_{z=0}$, $\tau_{wy} = \mu_{nf}\left(\frac{\partial v}{\partial z}\right)_{z=0}$, the wall heat flux from the stretching surface $q_w = -k_{nf}(1+R)\left(\frac{\partial T}{\partial z}\right)_{z=0}$ and wall mass flux from the stretching surface $q_m = -D_B(1+R)\left(\frac{\partial C}{\partial z}\right)_{z=0}$.

In terms of dimensionless variables are given by the local skin friction co-efficient about x-axis C_{fx} and y-axis C_{fy}, local Nusselt number Nu_x and local Sherwood number Sh_x

$$\mathrm{Re}_x^{1/2} C_{fx} = \frac{1}{(1-\phi)^{2.5}} f'(0) \quad , \quad \mathrm{Re}_y^{1/2} C_{fy} = \frac{1}{\lambda^{3/2}(1-\phi)^{2.5}} g'(0) \quad , \quad \mathrm{Re}_x^{-1/2} Nu_x = -A(1+R)\theta'(0) \quad \text{and}$$

$$\mathrm{Re}_x^{-1/2} Sh_x = -(1+R)C'(0) \tag{17}$$

Table1: Thermophysical properties of regular fluid and nanoparticles.

Physical properties	Regular fluid (water)	Cu (Copper)
C_p (J/kg K)	4179	385
ρ (kg/m^3)	997.1	8933
κ (W/mK)	0.613	400
$\beta \times 10^{-5}$ (1/K)	21	1.67

2. RESULTS AND DISCUSSION

A numerical study has been performed to draw out the variations in the flow pattern of Casson nanofluid past a stretched porous sheet in conducting field. To analyze velocity, temperature and concentration profiles, the parameters like thermal radiation, heat generation, radiation absorption, diffusion thermo effect, chemical reaction are also taken into account with the volume fraction $\phi = 0.01$ for Cu-water nanofluids. To confirm the accuracy a comparison is made by the present results with the results by Nayak [11]. A good conformity is observed in fig 6.

Figure 1 shows the variations of permeability of porous medium and Casson parameter on primary velocity. It is clear that the primary velocity decreases with the increase in porous medium parameter of the fluid due to enhancement of the viscosity of the fluid or decrease in the stretching rate of the acceleration on the surface and also the primary velocity decreases for the increasing values of Casson parameter. The effect of porous medium and

Casson parameter on secondary velocity is displayed in the figure 2. The secondary velocity increases with the increase in porous medium parameter whereas secondary velocity decreases for the increasing values of Casson parameter. Table 2 illustrates the variations in skin friction coefficient, Nusselt number and Sherwood number for various values of porous medium and Casson parameter.

Figure 3 states the effect of Prandtl number and heat generation parameter on temperature. It is clear that temperature decreases for the increasing values of Prandtl number. An increase in the Prandtl number reduces the thermal boundary layer thickness. It is seen that an increase in heat generation parameter leads to increase in the temperature. The changes in skin friction coefficient, Nusselt number and Sherwood number for increasing values of Prandtl number is displayed in the table 2. The effect of Soret number and chemical reaction parameter is represented in figure 4. It depicts that chemical reaction parameter decreases the concentration profiles where as an increase in the Soret number increases the concentration profiles.

The effect of Schmidt number and chemical reaction parameter on concentration is shown in figure 6. Schmidt number is a dimensionless number defined as the ratio of momentum diffusivity and mass diffusivity. It is clear that the concentration increases with the increase in Schmidt number. The effects of skin friction coefficient, Nusselt number and Sherwood number with the enhancement of Schmidt number are shown in table 2.

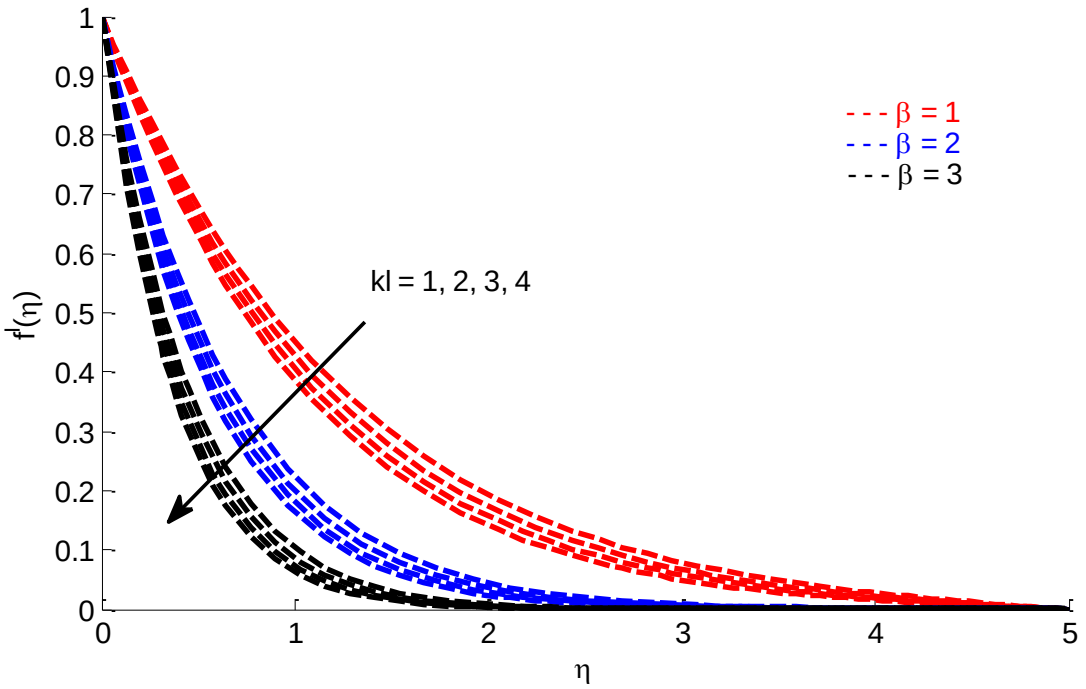

Fig 2. Primary velocity profiles for various values of porous medium parameter and Casson parameter.

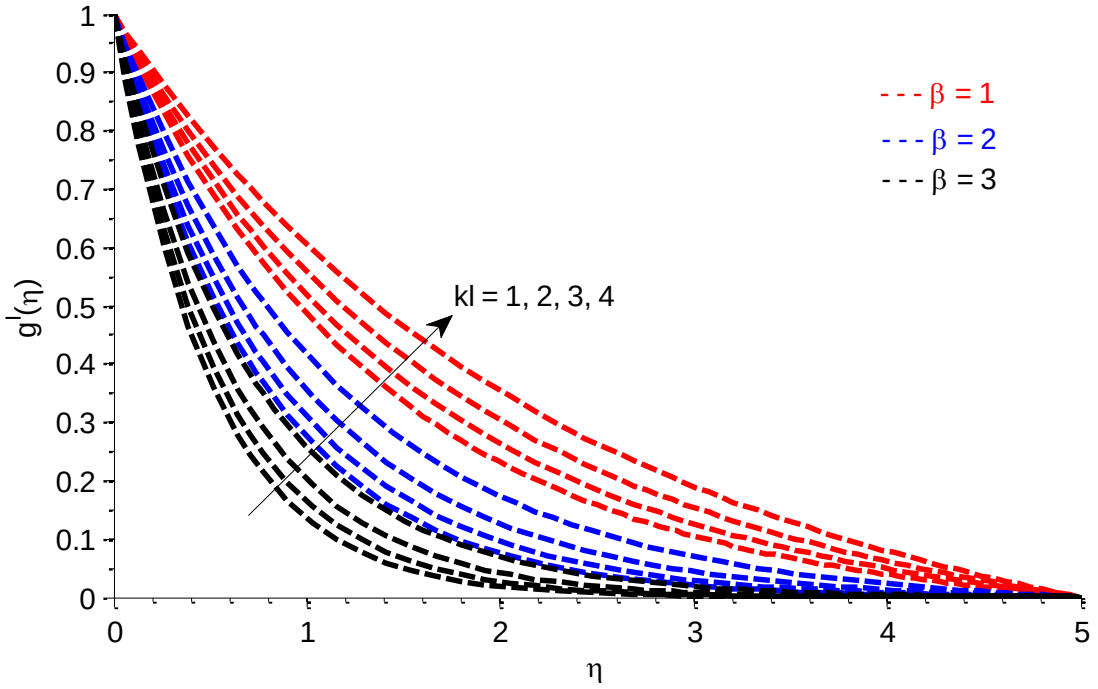

Fig 3. Primary velocity profiles for various values of porous medium parameter and Casson parameter

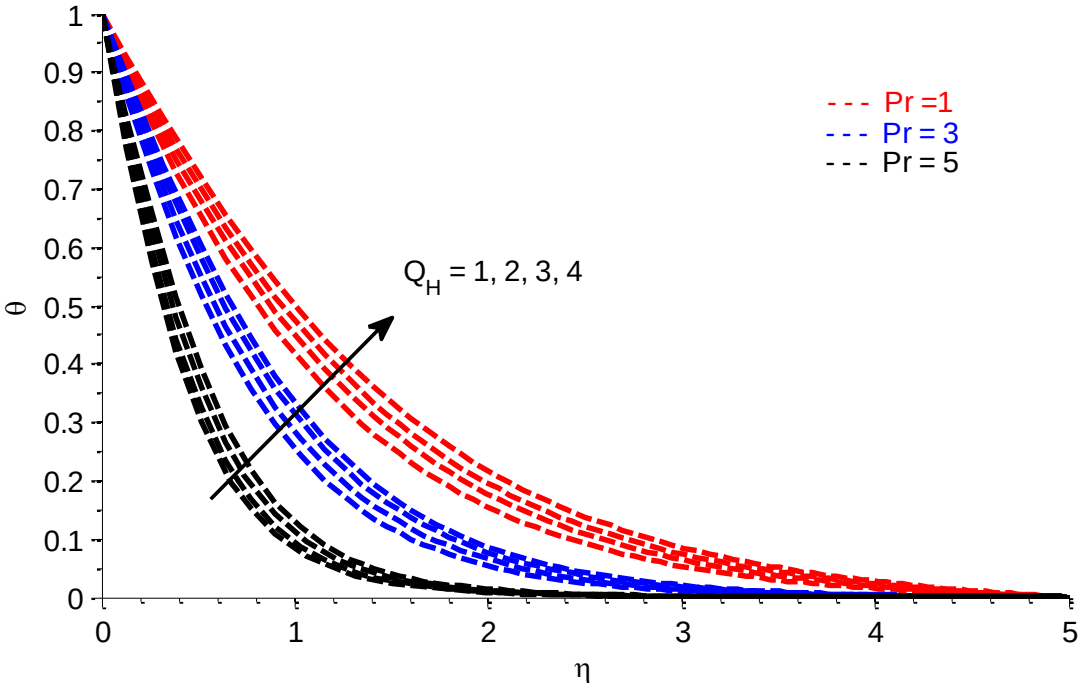

Fig 4. Temperature profiles for various values of heat generation parameter and Prandtl number

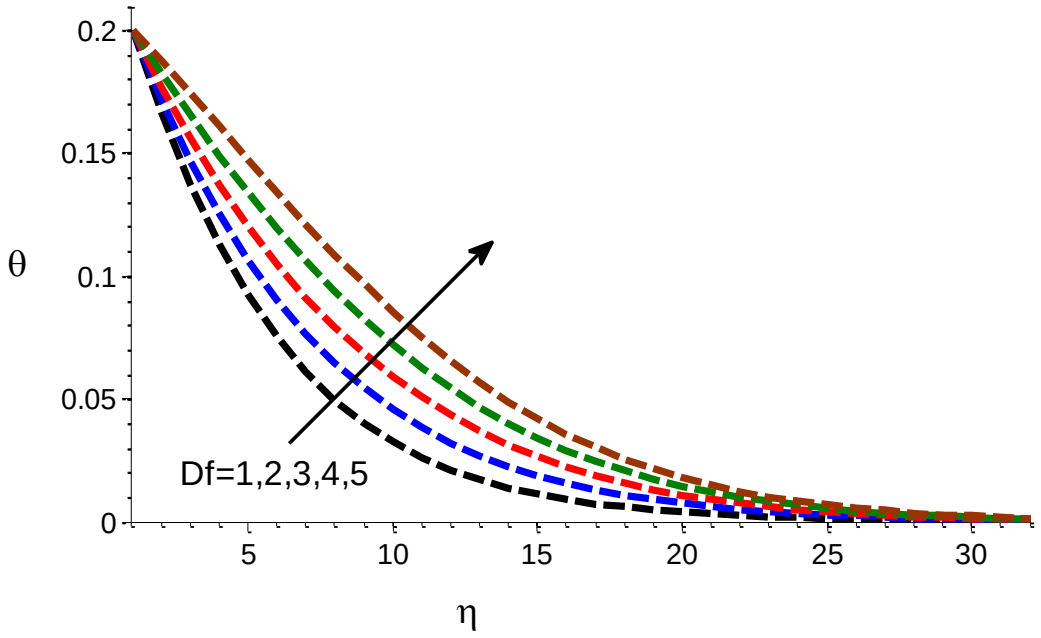

Fig 5. Temperature profiles for various values of Dufour number

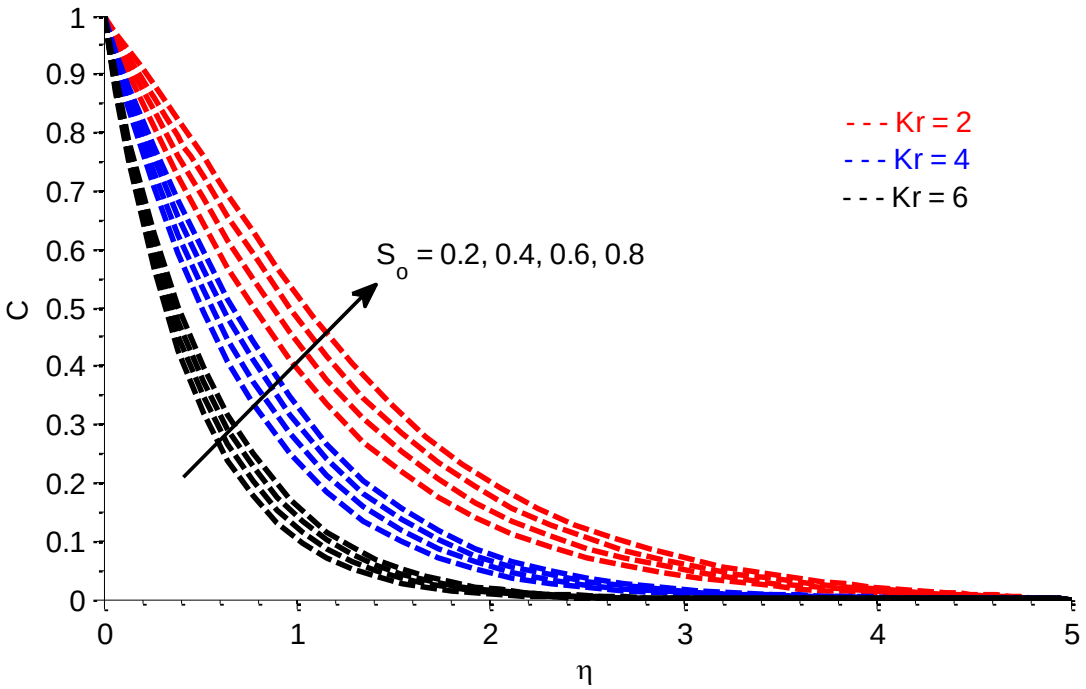

Fig 6. Concentration profiles for various values of Soret number and Chemical reaction parameter

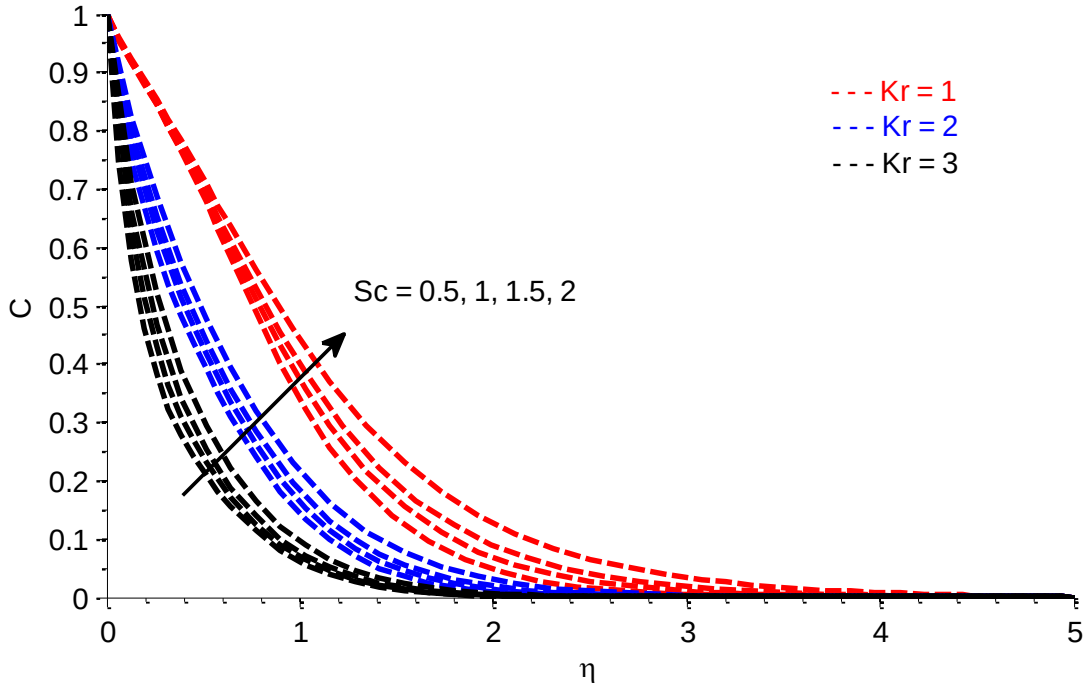

Fig 7. Concentration profiles for various values of Schmidt number and Chemical reaction parameter

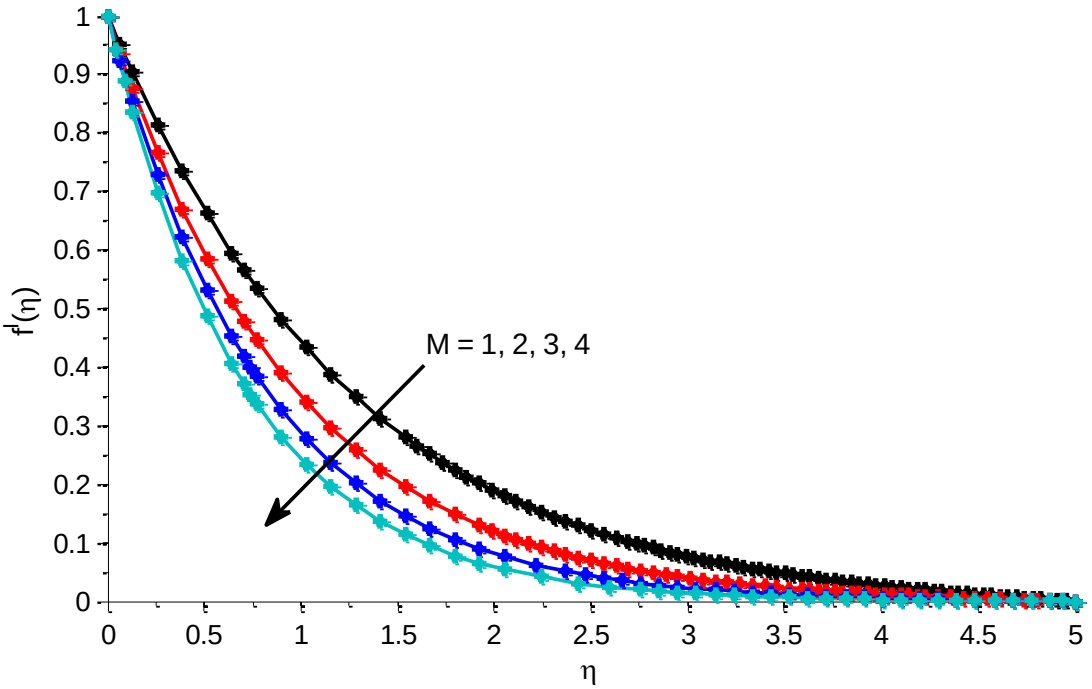

Fig 8. Comparison of primary velocity profiles for various values of Magnetic parameter in the presence and absence of Casson parameter and Dufour effect.

Table2: Skin friction, Nusselt number and Sherwood number for various values of magnetic parameter, radiation parameter, Schmidt number, stretching ratio parameter and Prandtl number.

R	Sc	Pr	kl	β	$\mathrm{Re}_x^{\frac{1}{2}} C_{fx}$	$\mathrm{Re}_x^{\frac{1}{2}} C_{fy}$	$\mathrm{Re}_x^{-\frac{1}{2}} Nu_x$	$\mathrm{Re}_x^{-\frac{1}{2}} Sh_x$
0.1	0.78	6.72	1	0.1	5.140155	-9.273021	0.010721	1.493261
0.2					5.146229	-9.271025	0.047918	1.600940
0.3					5.153249	-9.269380	0.085156	1.708444
0.4					5.160982	-9.268017	0.122354	1.815839
0.1	0.1				8.280679	-9.454326	-0.726268	0.547785
	0.2				7.337017	-9.403679	-0.509991	0.753136
	0.3				6.682429	-9.367103	-0.358259	0.920441
	0.4				6.201483	-9.339182	-0.245324	1.063855
	0.78	3			5.386029	-9.262510	1.021190	4.622536
		5			5.511043	-9.265077	1.638921	6.807938
		6.72			5.590133	-9.267227	2.142166	8.698359
		7.1			5.604967	-9.267659	2.250986	9.116945
		6.72	0.1		8.325454	-9.821725	0.247433	1.378502
			0.2		7.952794	-9.762121	0.220805	1.391476
			0.3		7.584766	-9.702192	0.194233	1.404409
			0.4		7.221389	-9.641932	0.167731	1.417293
			1	0.1	5.140155	-9.273021	0.010721	1.493261
				0.2	2.600976	-6.782319	0.135510	1.435817
				0.3	1.669990	-5.725076	0.195582	1.408946
				0.4	1.190306	-5.118105	0.236459	1.390791

3. CONCLUSION

To analyze the flow pattern of Casson nanofluid a numerical study has been performed past a stretched sheet in a conducting field. The governed ordinary differential equations are solved by shooting method using MAT Lab. The variations of velocity profiles, temperature profiles, concentration profiles, Skin friction coefficient, Nusselt number and Sherwood numbers are studied through graphs and tables. The following are the conclusions drawn from the present study.

- The primary velocity profile descends for the enhanced values of porous medium parameter and Casson parameter.
- The secondary velocity profiles enhance with the increasing permeability of the porous medium whereas it decline with the enhancement of Casson parameter.
- With an increase in Prandtl number, the temperature decrease whereas the temperature increases for the increasing values of heat generation parameter.
- The concentration profiles enhance with the enhancement of Schmidt parameter. The skin friction coefficient, Nusselt number and Sherwood number increases with an increase in radiation parameter.

4. REFERENCES

1. Choi S.U.S, Enhancing Thermal Conductivity of Fluids with Nanoparticles, Developments and Applications of Non-Newtonian Flows. FED-231/MD-vol (66) (1995) 99–1053.
2. Choi, S.U.S., Zhang, Z. G., Yu, W., Lockwood, F. E., Grulke, E. A., "Anomalous Thermal Conductivity Enhancement in Nanotube Suspensions," Applied Physics Letters, 79, (2001). 2252. http://dx.doi.org/10.1063/1.1408272
3. Hamad M.A.A.,"Analytical Solution of Natural Convection Flow of a Nanofluid over a linearly Stretching Sheet in the Presence of Magnetic Field," International Communications in Heat and Mass Transfer,

38(4), 2011, 487-492. http://dx.doi.org/10.1016/j.icheatmasstransfer.2010.12.042

4. Khan M. S., Alam M. M., Ferdows M, "Effects of Magnetic Field on Radiative Flow of a Nanofluid Past a Stretching Sheet," Procedia Engineering, 56, 2013,316-322, http://dx.doi.org/10.1016/j.proeng.2013.03.125
5. Nayak M.K., Akbar N.S., Tripathi D., Pandey V.S., "Three Dimensional MHD Flow of Nanofluid over an Exponential Porous Stretching Sheet with Convective Boundary Conditions," Thermal Science and Engineering Progress,3,133-140,2017. https://doi.org/10.1016/j.tsep.2017.07.006
6. Hayat, T., Muhammad, T., Shehzad, S.A., and Alsaedi, A., 2015, "Soret and Dufour Effects in Three-dimensional Flow over an Exponentially Stretching Surface with Porous Medium, Chemical Reaction And Heat Source/sink," Int. J of Numerical Methods for Heat & Fluid Flow, 25(4), 762 – 781. http://dx.doi.org/10.1108/HFF-05-2014-0137
7. Rosseland S., Astrophysik und atom-theoretische Grundlagen, Springer-Verlag, Berlin,1931.
8. Sheikholeslami M, GorjiBandpy M, Ellahi R., Zeeshan A, "Simulation of MHD CuO–water Nano fluid Flow and Convective Heat Transfer Considering Lorentz Forces," Journal of Magnetism and Magnetic Materials, 369, 69-80,2014. http://dx.doi.org/10.1016/j.jmmm.2014.06.017
9. Aurang Zaib, *et al.*, Numerical solution of second law analysis for MHD Casson nanofluid past a wedge with activation energy and binary chemical reaction,", International Journal of Numerical Methods for Heat & Fluid Flow, Vol. **27** Issue: 12, pp. 2816–2834, https://doi.org/10.1108/HFF-02-2017-0063
10. Hayat T, Imtiaz M, Alsaedi A, Mansoor R (2015) Magnetohydrodynamic three-dimensional flow of nanofluid by a porous shrinking surface. J. Aerospace Eng. 29, (2), doi: 10.1061/(ASCE)AS.1943-5525.0000533
11. Nayak M .K, Noreen Sher Akbar, Pandey V.S, Zafar Hayat Khan, Dharmendra Tripathi, 3D free convective MHD flow of nanofluid over permeable linear stretching sheet with thermal radiation, Powder Technology.315(2017)205-215,2017, DOI: 10.1016/j.powtec.2017.04.017
12. Aurang Zaib, *et al.*, Numerical solution of second law analysis for MHD Casson nanofluid past a wedge with activation energy and binary chemical reaction,", International Journal of Numerical Methods for Heat & Fluid Flow, Vol. **27** Issue: 12, pp. 2816–2834, https://doi.org/10.1108/HFF-02-2017-0063
13. Panigrahi, Lipika; Panda, Jayaprakash; Swain, Kharabela; and Dash, Gouranga Charan (2020) "Heat and mass transfer of MHD Casson nanofluid flow through a porous medium past a stretching sheet with Newtonian heating and chemical reaction," *Karbala International Journal of Modern Science*: Vol. 6 : Iss. 3 , Article 11. Available at: https://doi.org/10.33640/2405-609X.1740
14. Besthapu, P. and Bandari, S. (2015) Mixed Convection MHD Flow of a Casson Nanofluid over a Nonlinear Permeable Stretching Sheet with Viscous Dissipation. *Journal of Applied Mathematics and Physics*, **3**, 1580-1593. doi: 10.4236/jamp.2015.312182.
15. Prasad, K.V., Vajravelu, K. and Datti, P.S. (2010) Mixed Convection Heat Transfer over a Non-Linear Stretching Surface with Variable Fluid Properties. International Journal of Non-Linear Mechanics, 45, 320-330. http://dx.doi.org/10.1016/j.ijnonlinmec.2009.12.003
16. Hassani, M., Tabar, M.M., Nemati, H., Domairry, G. and Noori, F. (2011) An Analytical Solution for Boundary Layer Flow of a Nanofluid Past a Stretching Sheet. International Journal of Thermal Science, 50, 2256-2263. http://dx.doi.org/10.1016/j.ijthermalsci.2011.05.015

17. Rana, P. and Bhargava, R. (2012) Flow and Heat Transfer of a Nanofluid over a Non-linearly stretching Sheet: A Numerical Study. Communications in Nonlinear Science and Numerical Simulation, 17, 212-226.
18. Hussain, T., Shehzad, S.A., Alsaedi, A., Hayat, T. and Ramzan, M. (2015) Flow of Casson-Nano Fluid with Viscous Dissipation and Convective Conditions: A Mathematical Model. Journal of Central South University, 22, 1132-1140.
19. Mustafa, M. and Khan, J.A. (2015) Model for Flow of Casson-Nano Fluid Past a Nonlinearly Stretching Sheet Considering Magnetic Field Effects. AIP Advances, 5, Article ID: 077148.